

Electronic Supplementary Information: Porous Graphene-Based Materials by Thermolytic Cracking

Deqin Fan,^{a,b} Ying Liu,^a Junpo He,^{*a} Yanwu Zhou^a and Yuliang Yang^a

Table S1. Number average diameters, D_n s, and distributions, PDI s, of PS-*in*-RGOs from statistics of OM.

PVP con. (%)	GO con. (%)	$D_n(\mu\text{m})$	PDI^d
1.60	0	- ^a	- ^a
0	0.01	- ^b	- ^b
0.53	0.01	5.78	1.140
1.00	0.01	4.98	1.148
1.60	0.01	3.53	1.165
2.20	0.01	2.81	1.203
1.60	0.25	3.17	1.165
1.60	0.50	3.24	1.349
1.60	0.01 ^c	3.65	1.188
1.60	0.25 ^c	2.93	1.170
1.60	0.50 ^c	3.10	1.426

^{a.} Unable to precisely be determined due to limited resolution of the optical microscopy.

^{b.} Serious coagulum observed.

^{c.} The data is from the samples after chemical reduction reaction.

^{d.} The average diameter D_n and polydispersity index PDI were calculated according to:

$$D_n = \sum_{i=1}^n d_i/n, D_w = \sum_{i=1}^n d_i^4 / \sum_{i=1}^n d_i^3, PDI = \frac{D_w}{D_n},$$

where n is the number of counted particles and d_i is the diameter of the individual particle.

Table S2. Raman intensity ratios of graphite, RGO and PS-*in*-RGOs.

Sample	I_D/I_G
Graphite	0.21
PS- <i>in</i> -RGO1	1.47
PS- <i>in</i> -RGO2	1.46
PS- <i>in</i> -RGO3	1.49
RGO	1.61

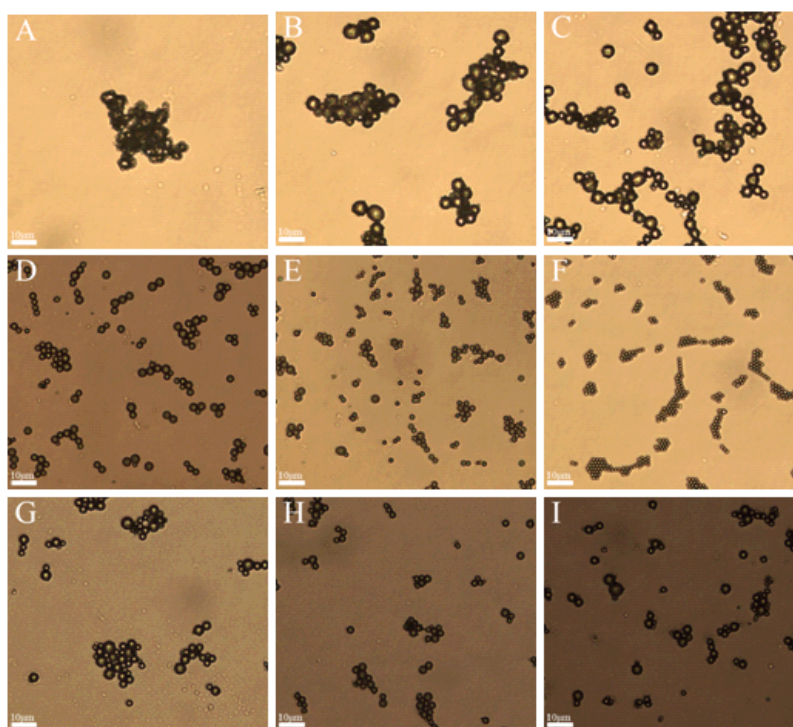


Fig. S1 Optical images of the PS-*in*-GO on glass slide with PVP concentration at (A) 0%, (B) 0.53%, (C) 1.06%, (D) 1.60%, (E) 2.20% at 0.01% GO; (F) standard control polystyrene microspheres; PS-*in*-RGOs with GO concentration at (G) 0.01%, (H) 0.25%, (I) 0.50% at 1.60% PVP. The scale bars are 10 μm .

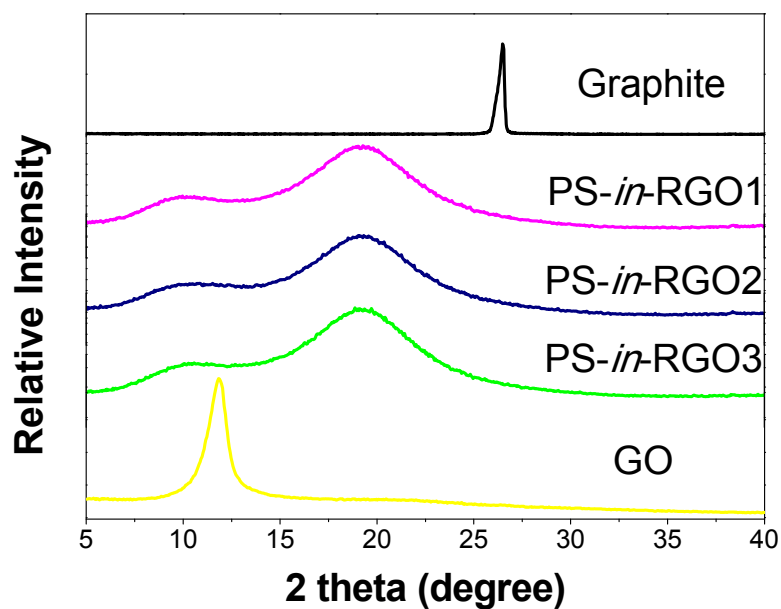


Fig. S2 XRD spectra of GO, PS-*in*-RGOs and graphite.

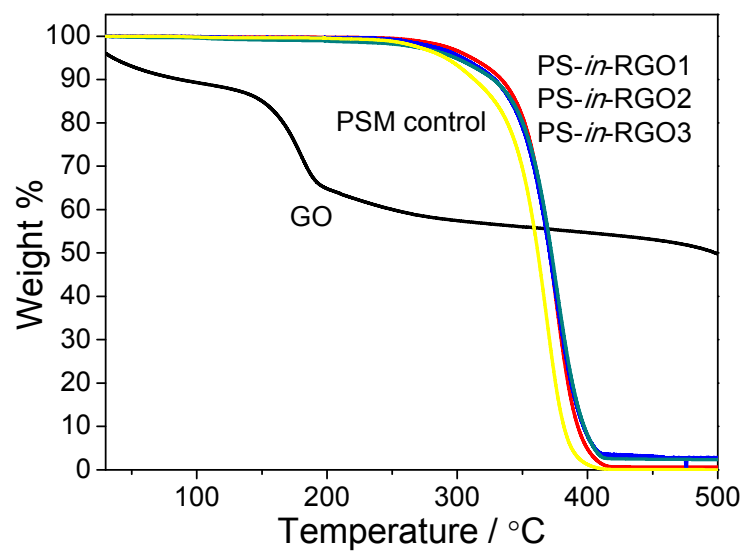


Fig. S3 TGA curves of GO, PS-*in*-RGOs and control polystyrene microspheres (PSM) prepared in the absence of GO.

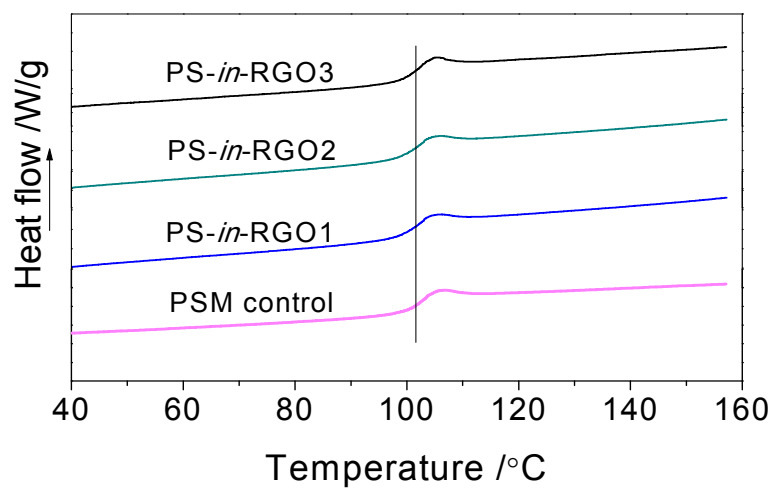


Fig. S4 DSC curves of PS-*in*-RGOs and control polystyrene microspheres (PSM) prepared in the absence of GO.

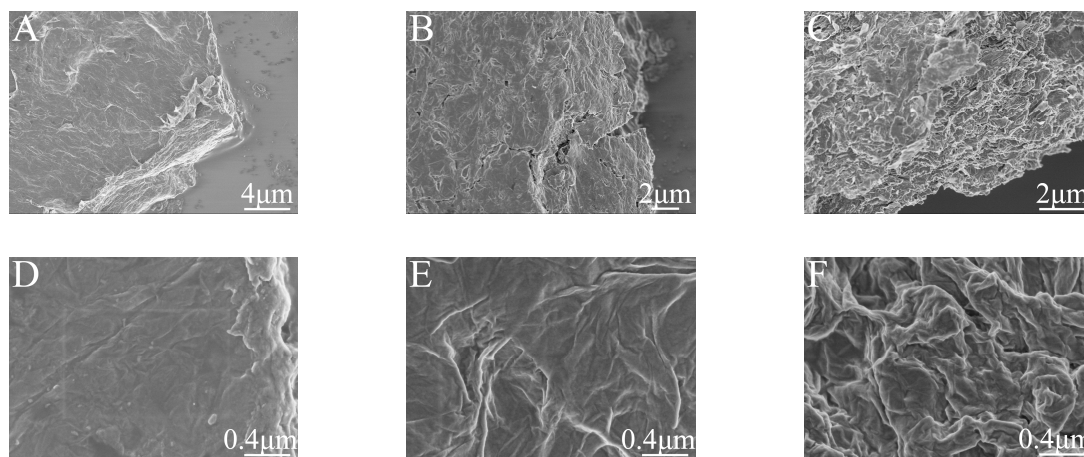


Fig. S5 SEM images of recycled RGO by solvent abstract of PS-*in*-RGO1 (A, D), PS-*in*-RGO2 (B, E) and PS-*in*-RGO3 (C, F).

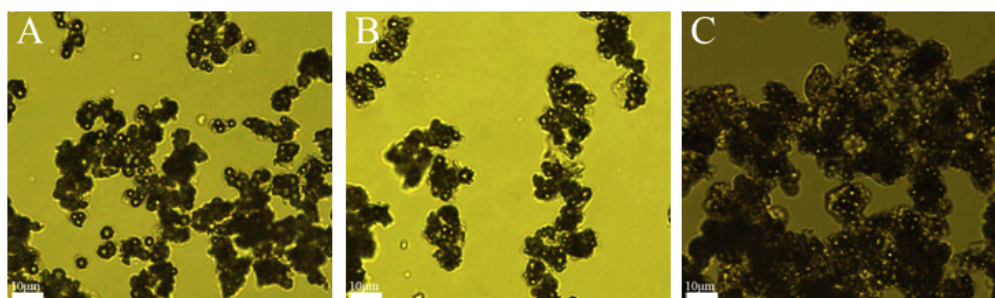


Fig. S6 Optical images of (A) PS-*in*-GO/SiO₂1, (B) PS-*in*-GO/SiO₂2 and (C) PS-*in*-GO/SiO₂3.

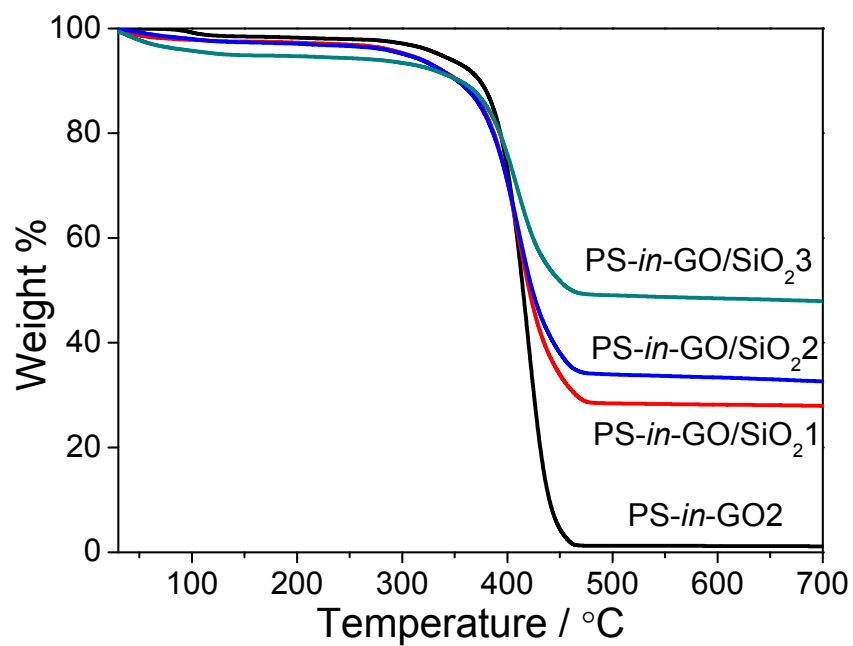


Fig. S7 TGA curves of (A) PS-*in*-GO₂, (B) PS-*in*-GO/SiO₂1, (C) PS-*in*-GO/SiO₂2 and (D) PS-*in*-GO/SiO₂3.